



Mercator - Revista de Geografia da UFC
ISSN: 1984-2201
mercator@ufc.br
Universidade Federal do Ceará
Brasil

GPR STRATIGRAPHY AND QUATERNARY MORPHOGENESIS IN THE SEMIARID BRAZIL

Teixeira de Oliveira, Marcelo Accioly; Santos, Janaina Carla

GPR STRATIGRAPHY AND QUATERNARY MORPHOGENESIS IN THE SEMIARID BRAZIL

Mercator - Revista de Geografia da UFC, vol. 18, no. 8, 2019

Universidade Federal do Ceará, Brasil

Available in: <https://www.redalyc.org/articulo.oa?id=273661094009>

GPR STRATIGRAPHY AND QUATERNARY MORPHOGENESIS IN THE SEMIARID BRAZIL

ESTRATIGRAFIA GPR E MORFOGÊNESE QUATERNÁRIA NO SEMIÁRIDO BRASILEIRO

STRATIGRAPHIE GPR ET MORPHOGENÈSE QUATERNAIRE DANS LE SEMIARIDE BRÉSILIEN

*Marcelo Accioly Teixeira de Oliveira ***Federal University of Santa Catarina,, Brasil**maroliv@cfh.ufsc.br*Redalyc: [https://www.redalyc.org/articulo.oa?](https://www.redalyc.org/articulo.oa?id=273661094009)

id=273661094009

*Janaina Carla Santos ***Universidade Federal do Vale do São Francisco, Brasil*

Received: 12 August 2019

Accepted: 11 October 2019

ABSTRACT:

The Serra da Capivara National Park is an optimal case study for Quaternary and geomorphology studies in the semiarid region of northeastern Brazil. Previous research in the Serra Branca valley, which is one of the park's main geomorphological units, reveals the predominance of thick colluvial deposits, suggesting episodic fluctuations towards wetter semiarid climates since the Upper Pleistocene. This study focuses on the application of GPR stratigraphy to Quaternary deposits along the three kilometers-wide middle reach of the Serra Branca valley. High-resolution GPR and RTK data and OSL dating suggest a more complex geomorphic evolution than previously envisioned. Results indicate the existence of gullied first-order watersheds that lie buried under small alluvial fan deposits since at least the Early to Middle Holocene. A 300 meters-wide alluvium filled paleo-channel is found, hanging about 14 meters higher than the present valley bottom and recording the incision of the valley since the Last Glacial Maximum. GPR and RTK data enable mapping truncated rock surfaces; colluvial and alluvial deposits; pediments; worn down watersheds; a relict fluvial channel, and the present valley bottom. Results suggest that the local climate during the last global glacial stage was wetter than today.

KEYWORDS: Semiarid, GPR, Stratigraphy, Morphogenesis, Quaternary, Serra da Capivara.**RESUMO:**

O Parque Nacional da Serra da Capivara desponta como estudo de caso para pesquisas do Quaternário e de geomorfologia no nordeste semiárido brasileiro. Trabalhos anteriores no vale da Serra Branca, uma das principais unidades geomorfológicas do parque, revelam o predomínio de espessos depósitos colúvies, sugerindo flutuações climáticas episódicas com aumento da umidade no semiárido desde o Pleistoceno Superior. Este estudo está focado na aplicação da estratigrafia GPR à investigação de depósitos quaternários nos três quilômetros de largura do médio-curso do vale da Serra Branca. Dados GPR e RTK de alta resolução e datações LOE sugerem evolução geomorfológica mais complexa do que a vislumbrada anteriormente. Resultados indicam bacias de primeira ordem com incisões erosivas soterradas por depósitos de leques aluviais datados do Holoceno Médio a Inferior. Paleo-canal de 300 metros de largura, preenchido por aluviões, ocorre suspenso a 14 metros acima do fundo do vale atual, documentando a incisão do vale desde Último Máximo Glacial. Os dados GPR e RTK possibilitam mapear rochas truncadas; depósitos colúvies e aluviais; pedimentos; divisores rebaixados; canal fluvial relictual, e o fundo do vale atual. Os resultados apontam para clima mais úmido do que o atual durante o último estágio glacial global.

PALAVRAS-CHAVE: Semiárido, GPR, Estratigrafia, Morfogênese, Quaternário, Serra da Capivara.**RÉSUMÉ:****AUTHOR NOTES**

* ORCID: <http://orcid.org/0000-0002-9145-4870>.
LATTES: <http://lattes.cnpq.br/4408742728972066>

* ORCID: <http://orcid.org/0000-0001-5341-6219>
LATTES: <http://lattes.cnpq.br/0113004052201333>

Le Parc National de la Serra da Capivara se distingue comme étude de cas pour des recherches du Quaternaire et de géomorphologie dans le nordeste semi-aride Brésilien. Étudespréalables dans la vallée de la Serra Branca démontrent la prédominance sur cette unité géomorphologique d'épais dépôts colluviaux, liés à desépisodes climatiques plus humides dans le semi-aride dès le Pléistocène Supérieur. Cette étude vise l'application de la stratigraphie GPR aux dépôts quaternairesde la moyenne vallée de la Serra Branca, large de trois kilomètres. Données GPR et RTK d'haute résolution et datations LOE suggèrent une évolution géomorphologique pluscomplexe que celle envisagée préalablement. Les vallées de premier ordre sont entaillées par des ravins, ensevelis sous des cônes alluviaux datés de l'Holocène Moyen aInférieur. Un paleo-chenal alluvial, large de 300 mètres, se trouve perché de 14 mètres sur le fond de vallée actuelle, enregistrant la dissection de la vallée dès le DernierMaximum Glacial. Les données GPR et RTK permettent de cartographier surfaces tronquées ; dépôts colluviaux et alluviaux ; pédiments ; lignes de faite aplanies ; un chenal fluvial relictuel,et le talweg actuel. Les résultats suggèrent un climat plus humide qu'aujourd'hui durant le dernier cycle glacial global. Mots-clés : Semi-aride ; GPR ; Stratigraphie ; Morphogenèse ; Quaternaire ; Serra da Capivara. INTRODUCTION

MOTS CLÉS: Semi-aride, GPR, Stratigraphie, Morphogenèse, Quaternaire, Serra da Capivara.

INTRODUCTION

The Serra da Capivara National Park (SCNP) displays landscapes of great scenic beauty in the Brazilian Caatinga (dry forest) biome. The park is internationally known for its archaeological sites, which indicate early human occupation in South America, and challenge prevailing views of Late Glacial propagation of humans through the Bering Strait. From a geomorphological perspective, the SCNP area is dominated by cuesta-likesandstone plateaus on which a consequent low-drainage density network develops along the dip slopes. Near the cuesta fronts, the structurally-controlled drainage evolve into canyons and deep gorges, which are locally framedby pillars, arches and cavities that are typical of ruinform landscapes carved out of sedimentary rocks.

Geomorphological maps available for the SCNP area classify the park's landscape in two geomorphological units (PELLERIN, 1984): a) sandstone plateaus; and b) cuestas; and three morphostructuralunits (SANTOS, 2007): a) the Serra Branca Valley; b) the Cuesta Dip Slope; and c) Structural Staircases. According to Pellerin (1984), the sandstone plateaus are located in the western portion of the SCNP, with their characteristiclow-dissected and gentle monoclinal tops. The plateaus' gentle topography is interrupted by deeply incised S-N oriented valleys, with flat bottoms framed by sandstone cliffs. The dip-slope plateaus shift northwards to more tabular landforms, where isolated residual buttes sit on structural staircases. Near the northern border of the park the valleys develop wide and flat bottoms, with badland-type gullies along the slopes.

In this work we focus on the Serra Branca Valley morphostructural unit, which is characterized as a consequent deeply entrenched S-N oriented valley with a flat bottom (SANTOS, 2007). The valley is located on the western edge of the SCNP and is supported by sandstones and conglomerates of the Canindé Group (CPRM, 2009). Due to the general configuration of surrounding dip-slope plateaus, the Serra Branca Valley has local base levels that range from 520 meters above sea level, at the headwaters, to approximately 400 meters downstream, with an incision amplitude of about 120 meters that is over 45 km in length.

Runoff produced within the valley is integrated to the Piauí-Canindé River sub-basin, which belongs to the Parnaíba River basin. Like the other tributaries from the right banks of the Parnaíba River, the Piauí River has a temporary torrential regime, with flash flows during the rainy season (PELLERIN, 1984). The Serra Branca Valley has no well-defined channel banks, across most of its extension; this impedes the precise identification of overland flow pathways. The main drainage lines are endoreic, and may be mapped only by areas of greener vegetation across the Caatinga. These areas develop after periods of precipitation, forming elongated and discontinuous zones of wetter subsoil, pointing to areas that have a higher probability of occurrence of subsequent intermittent overland flow (DUNNE and BLACK, 1970; MONTGOMERY and DIETRICH, 1988). Only near the valley outlet, towards the North, do these wetter soil zones acquire a better linear aspect, although with no clear channel. Due to the rarity of channelized runoff, sediment

transport occurs according to a discontinuous, anastomosed pattern, and sediments are transferred by intermittent flash flows under the caatinga vegetation, forming discontinuous and shallow lobes of washed sands with no apparent sedimentary structures (PETTIJOHN et al., 1987).

Previous quaternary studies at the Serra Branca site describe coarse colluvial and talus deposits near the cliffs that border the valley. Deposits and associated saprolites are transferred down the valley, forming colluvial layers and colluvial-alluvial fans that may coalesce and overlay gentle pediments dipping to the valley bottom (SANTOS, 2007). The thickness of the quaternary deposits ranges from 3.20 to 12.00 meters. They are either composed of alternating layers of yellowish sands and concentrations of sandstone fragments, or of layers of massive yellowish sands and gravels (SANTOS; BARRETO; SUGGES, 2012). Alluvial sediments eventually present across the flat valley bottom have not been previously studied. Their total thickness is unknown, as well as their relationship with colluvial deposits and the main geomorphological features of the valley (fans, ramps, pediments, watersheds and buttes).

Considering the above descriptions, the Serra Branca valley bottom is a gentle, flattened topographic surface that is surrounded by prominent sandstone cliffs, composing an image that recalls the original definition of pediments and pediplanes (GILBERT, 1877; KING, 1953). The study of pediments and pediplanes in Brazil was inaugurated by the groundbreaking work of J.J. Bigarella and his collaborators, giving rise to several approaches for characterizing pediments and pediplanes (BIGARELLA; MOUSINHO; SILVA, 1965). Despite eventual controversies, however, it remains well-established that pediments and pediplanes are common features in landscapes that are under the influence of arid and semi-arid climates (TWIDALE, 1983; TWIDALE; BOURNE, 2013).

In the Brazilian semiarid, few studies show a clear association between Quaternary deposits and typical landforms of arid and semiarid climates, such as pediments, pediplanes, alluvial fans, etc. In this context, the SCNP emerges as a geomorphological case study of choice within the Caatinga biome, revealing a sedimentological record that demonstrates the resilience of semiarid climate systems, with wet fluctuations, between the Upper Pleistocene and the Holocene (SANTOS; BARRETO; SUGUIO, 2012). This resilience is corroborated by palynologic, isotopic, and paleontological records from the Brazilian semiarid that are difficult to conciliate to the bipolar paradigm that is usually associated with the effects of global glaciations in Brazil (OLIVEIRA et al., 2014).

This paper results from research programs that applied Ground Penetrating Radar (GPR) to the study of the shallow stratigraphy of Quaternary deposits in the SCNP area. We present results from surveys across the middle-course of the Serra Branca valley, where Quaternary sedimentary layers and truncated topographic surfaces were found in association with levelled watersheds, pediments, and perched valley bottoms. Together with the application of optically stimulated luminescence (OSL) dating, the study's geophysical approach enables: a) the identification and characterization of shallow subsurface structures across the valley; b) the definition of erosion and sedimentation rates for studied sites across the valley; and c) the formulation of hypotheses accounting for the role of incision and backwearing processes on the evolution of the valley bottom, based upon stratigraphic, geophysical and geochronological records.

Unlike what is commonly reported for sites of similar morphology in desertic areas, whose geomorphologic evolution occurs on scales of tens of thousands and hundreds of thousands of years (10⁴ to 10⁵ years), the middle-course of the Serra Branca valley yields abundant evidence of relatively shorter and recent episodes of erosion and deposition. The results point to the adaptation of the drainage network and of local landforms to events that range from the Upper Pleistocene to the Holocene, on time scales of the order of thousands to tens of thousands of years (10³ to 10⁴ years).

STUDY AREA

The Serra da Capivara National Park (SCNP) was created in 1979 in the southeast of the Brazilian state of Piauí (Figure 1). The park encompasses part of the municipalities of Brejo do Piauí, João Costa, São Raimundo Nonato and Colonel José Dias, defining a territory of 129,953 ha within a perimeter of 214,235.37 meters of protected area. The SCNP was classified by UNESCO (the United Nations Educational, Scientific and Cultural Organization) as a World Cultural Heritage site, in 1991. (PROCHOROFF; BRIGHT, 2015).

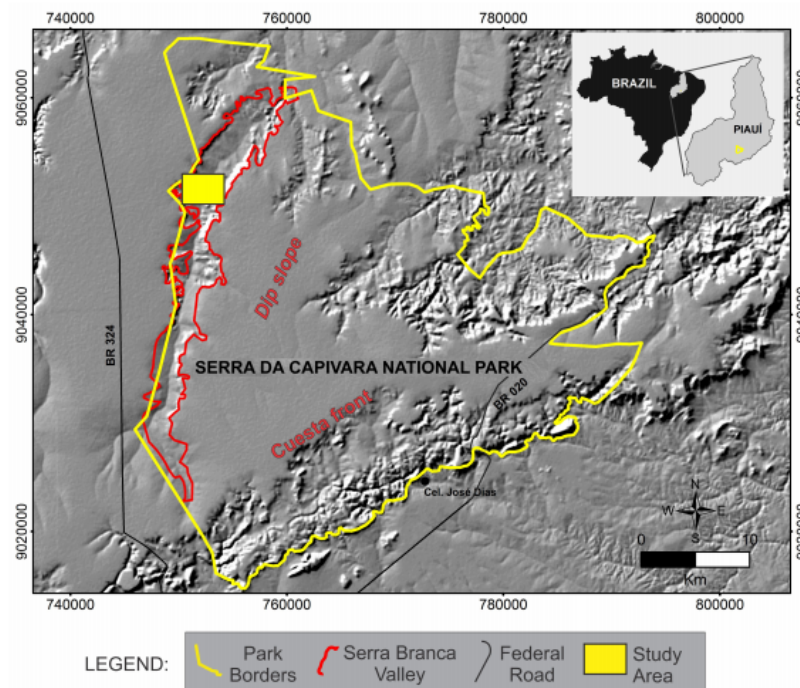


FIGURE 1

tudy area location. Database: IBGE / ICMBio / DNIT. Digital terrain model source: www.relevobr.cnpm.embrapa (accessed in 10/11/2017). Metadata: UTM, Sirgas 2000, 23 S. Produced by Reginaldo Lemos.

The climate in the SCNP region is of the BShw type: semi-arid, hot, with rainy summers. The average annual temperature is about 28 °C, with a rainy season that lasts from October to April, although varying interannually. The average precipitation is 689 mm per year, with a standard deviation of 200 mm, and a modal class between 600 and 700 mm per year (EMPERAIRE, 1980). Local vegetation is composed of Caatinga (dry forest), with typical vegetal associations of the northeastern Brazilian semiarid, occurring within the SCNP area as high and dense shrub caatinga; arboreal formations; medium and dense arboreal caatinga; low shrub caatinga, and shrub and arboreal caatinga.

The geomorphology of the park is characteristic of landscapes developed at the border of raised sedimentary basins, with landforms reflecting the monoclinical attitude of sedimentary rocks. Landforms and vegetation develop on a substrate dominated by the marginal portion of the Parnaíba Sedimentary Basin that covers part of northeastern and northern Brazil. This is a sedimentary basin, which is mostly Paleozoic in age, although Mesozoic deposits also occur on considerable areas (MESNER; WOOLDRIDGE, 1964).

Across the areas surrounding the SCNP, the main rock outcrops belong to the Casa Nova, Serra Grande and Canindé groups, respectively attributed to the Cryogenic (Neoproterozoic), Silurian and Devonian periods. The description of the stratigraphy of these groups may be found on the stratigraphic

column of Góes and Feijó (1994). The Casa Nova Group consists of the Barra Bonita Formation and the Intrusive Suite Serra da Aldeia. The Barra Bonita Formation is found at the southeastern limit of the park, with Neoproterozoic metamorphic rocks, such as schists, gneisses, phyllites and metalimestones (BARBOSA, 2012). The Serra Grande Group consists of the Ipu, Tianguá and Jaicós formations, which are associated with the first marine transgression reported for the Parnaíba Basin (CUNHA, 1986). The Canindé Group is composed by the Itaim, Pimenteiras, Cabeças, Longá and Poti formations (GÓES; FEIJÓ, 1994). These rocks were deposited during a stage of subsidence, and are associated with the largest marine transgression recorded in the Parnaíba Basin (VAZ et al., 2007).

Within the SCNP, rocks of the Barra Bonita Formation (Casa Nova Group) occur only at the park's southeastern border. The stratigraphy is continued by rocks of the Ipu Formation (Serra Grande Group), and the Itaim, Pimenteiras and Cabeças formations (Canindé Group). The Ipu Formation consists of sandstones, conglomerates, conglomeratic sandstones and diamictites formed at the beginning of the Silurian, under the influence of a braided fluvial environment (VAZ et al., 2007). The Itaim Formation dates from the Devonian, and displays light-colored fine sandstones and gray shales from a platform deltaic environment under tidal and storm influences (GÓES; FEIJÓ, 1994). The Itaim Formation overlaps the Ipu Formation in angular unconformity (BARROS et al., 2011). We note, however, that there is no detailed map either proving the presence of the Itaim Formation (Canindé Group) or providing accurate information about the Serra Grande Group formations within the SCNP area.

The Pimenteiras Formation consists of thick layers of dark gray and black shales, alternated with sandstones and siltstones, and with associated ferruginous mineral nodules. Della Fávera (1990) interprets these rocks as the products of an infra-neritic to coastal environment, under the influence of swells. This formation outcrops along the cuesta front, where its lower units are exposed, with fine micaceous sandstones and locally conglomeratic and calciferous sandstones set in plane parallel stratification (BARROS et al., 2011).

Specifically at the study area, within the Serra Branca valley, mapped rocks belong to the Cabeças Formation (Canindé Group) (CPRM, 2009). They consist of medium to coarse light-brown, cross-stratified sandstones, intercalated with stratified siltstones and shales that are associated with proximal-tidal lobes, transitioning into tempestites, and micaceous siltstones and shales in distal sections (DELLA FÁVERA, 1990). Glaciogenic diamictites occur to the top, associated with the Neodevonian unconformity that marks the transition between the sandstones of the Cabeças Formation and the shales of the Longá Formation (FERRAZ; CÓRDOBA; SOUZA, 2017). Cenozoic clast-lateritic deposits complete the local stratigraphy.

There is no evidence of the Mesozoic deposits of the Parnaíba Basin reported for the study area. Pellerin (1984) have studied the Cenozoic deposits of this basin, defining four units for the SCNP and surrounding areas. Only one of these units occurs within the park, according to the author, the "Superficial Formations, composed by saprolites and soils". Santos, Barreto and Suguio (2012) attribute a Holocene age to these superficial formations, as indicated by OSL dating.

MATERIALS AND METHODS

THE methodology adopted for this study involved the application of GPR data to the analysis of Quaternary deposits in continental environments (Oliveira et al. 2012). GPR data were obtained through a Geophysical Survey Systems Inc (GSSI) acquisition system that is set for 200 MHz monostatic-shielded antennas. Data was acquired through common-offset geophysical reflection surveys, and the resulting GPR signal was post-processed according to a standard protocol, which focuses on the increase of the signal-to-noise ratio by the application of high-pass and low-pass frequency filters; time-variant scale gain; Kirchhoff migration, and topographic correction. Post-processing methods are performed on RADAN 7.0[®] and ReflexW 3[®] softwares.

While in the field, the preliminary results from the GPR survey allowed the selection of specific sites for subsurface prospection, through manual auger drillings and the excavation of pits, to supply ground-truth data for further interpretation. Especially in the pits, the main characteristics of sediments and rocks are observed. The depths of transitions within unconsolidated sediments and between sediments and sedimentary rocks are carefully recorded, as ground-truth data.

The comparative analysis of ground-truth and GPR data in line-scans (radargrams), allows calculating dielectric constants that permit transforming the two-way-travel-times of electromagnetic pulses (EM) into average velocities of propagation through the medium. From this step the radargrams may be analyzed at average depths. Data interpretation is based on the association of the GPR signal with stratigraphic and sedimentological characteristics.

The values calculated of dielectric permittivity (dielectric constant) vary, from site to site, ranging between 7.86 and 2.88 farad (F) per meter. Based on these values, calculated average velocities for propagation of EM waves through the subsoil vary, respectively, from 0.10 to 0.17 m.ns⁻¹. Considering the dominant return-frequencies recorded in the radargrams and the calculated velocities of propagation, the vertical resolution of our data ranges between 5 and 9 cm, attaining equivalent depths between 4 and 10 meters below the topographic surface, according to the site.

These parameters allow interpreting the GPR data according to the general principles of radar stratigraphy, which are based on the analysis of the GPR reflectors, accounting for the spatial distribution; lateral continuity, and magnitude of the reflectors. GPR reflectors are created by the passage of EM pulses through materials with different physical properties. In the case of stratigraphic environments, GPR reflectors occur in association with the transition of physically distinct sedimentary layers. As a result, the geometry of relatively continuous reflectors is a proxy for the geometry of transitions between sedimentary layers, allowing stratigraphic interpretation. Detailed characteristics of GPR reflectors are observed within packages of reflectors, expressing the eventual occurrence and spatial distribution of detailed sedimentary structures, and supporting the interpretation of radar-facies.

To obtain the precise spatial positioning of GPR survey lines, we performed a Real Time Kinematic (RTK) topographic survey, with Trimble R6 GNSS equipment, composed of a fixed GPS receiver and a rover receiver, providing real-time positioning along the GPR survey lines. The system was set to acquire data at a 3-seconds rate, enabling the acquisition of georeferenced topographic profiles along survey lines. Raw data were postprocessed for geodesic correction, and to transform UTM coordinates into linear coordinates, providing topographic profiles for every GPR radargram. The resultant altimetric data was applied to the topographic correction step of GPR post-processing methods, allowing a more realistic interpretation of the geometry of the radargram and its detailed reflectors, and enabling the association of GPR data, stratigraphy and detailed landforms.

To establish a temporal framework for the studied deposits, samples were collected within pits for Optically Stimulated Luminescence (LOE) dating, following standard procedures to avoid partial bleaching caused by exposure to sun-light. The samples were processed and dated by the company “Datação, Comércio e Prestação de Serviços Ltda, São Paulo, Brazil”, using the SAR method, with 15 aliquots. Supplementary samples were collected within the pits and by auger drillings to define the main properties of the subsoil surveyed.

RESULTS AND DISCUSSION

Figure 2 presents the location of the studied sites, along with some general aspects of the surveyed area. The GPR survey-lines are also indicated, accounting for about 4,000 meters of GPR and RTK data, with ground-truth data sites shown at specific locations. Due to the significant extension of the survey lines and the shallow range of GPR data, specific segments of the survey lines were selected, in which some arbitrary vertical

scale exaggeration was applied when needed, to illustrate the main geophysical, structural and stratigraphic characteristics of the sites studied.

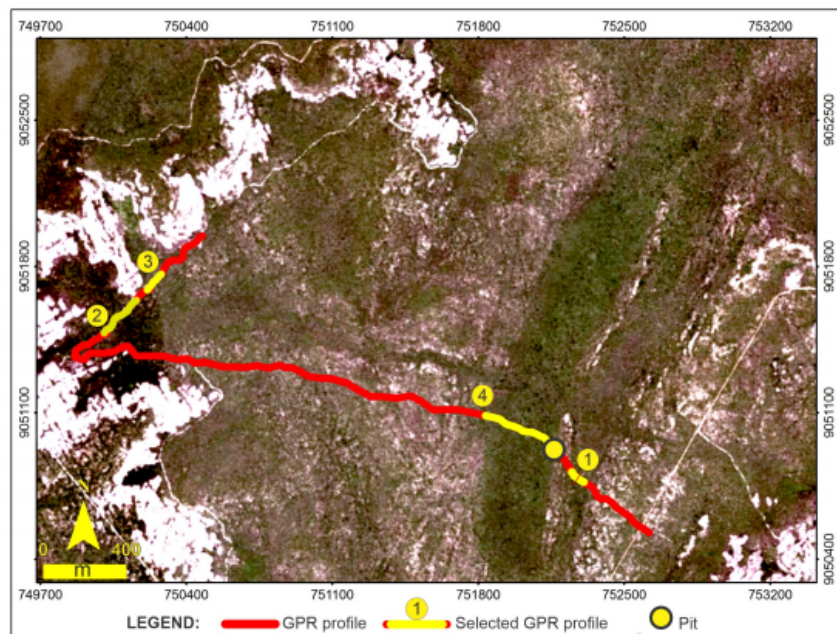


FIGURE 2

Detailed study area. The numbered circles refer to selected segments of GPR survey lines for this study (yellow lines). The order of numbers corresponds to the order of presentation of results in the main text. Data source: www.relevobr.cnpm.embrapa (accessed in: 10/11/2017). Metadata: UTM, Sirgas 2000, 23 S. Figure produced by Reginaldo Lemos.

GPR reflection pattern, structure of the subsoil and Quaternary recent deposits

The pattern of the GPR reflection across the survey area enables differentiating two types of subsoil materials. The first are materials with low relative magnitude geophysical reflectors that are also poorly organized in space (weak lateral continuity and poor orientation). The second relates to materials whose reflectors have a strong relative magnitude and good spatial organization (Figure 3). The former is associated with unconsolidated quaternary sediments, and the latter with local sedimentary rocks. In some specific cases, such as in the vicinity of topographic drainage troughs (Figure 3), quaternary sediments may develop stronger magnitude and well-organized reflectors, also indicating the better organization of deposits in layers with distinct physical properties.

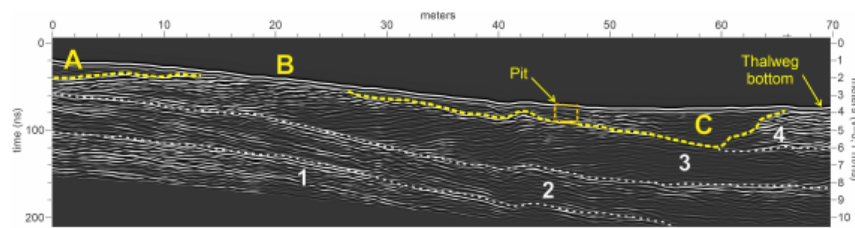


FIGURE 3

200 MHz radargram, with no vertical exaggeration, crossing the axis of the Serra Branca valley current thalweg (GPR line number 1 in Figure 2). A and C: typical examples of the reflection pattern defined in this study for recent sediments. B: reflection pattern of sedimentary rocks, either outcropping or in subsurface. White numbers indicate generic allostratigraphic units for the local Paleozoic rocks. Note: i) the inner GPR reflectors of allostratigraphic unit 3, organized as mega-ripple marks that are partially truncated by the topographic surface, at B; ii) the asymmetric channeled subsurface structure in C (yellow dashed line); iii) the location of the bottom of the current thalweg, where another rock outcrop occurs (unit 4); iv) location of a pit that confirms the depth of the transition between bedrocks and recent sediments.

The Quaternary sediments in this study generally occur in unconformity over Paleozoic sedimentary rocks. At the transition between sedimentary rocks and unconsolidated sediments, terminations of the well-defined and high-magnitude reflectors often occur in tolap (Figure 3). Unconformities between these materials characterize Quaternary surfaces of truncation across the surveyed area, occurring mostly in association with rock outcrops and shallow deposits (20 and 200 cm deep).

Besides the above distinction of the GPR reflection pattern in sediments and rocks, the quaternary deposits can be classified into two different groups, according to the velocity of propagation of EM pulses through sediments. The first group corresponds to materials that induce average velocities of propagation of about 0.10 m.ns⁻¹. These materials have variable thicknesses, predominantly composed of medium to fine massivesands, with incipient pedogenesis. The second group is composed of materials that have average velocities of propagation close to 0.17 m.ns⁻¹. These sediments have equally variable thicknesses and are formed by massive coarsesands that alternate with beds of locally well-stratified fine gravels (granules and pebbles). As an effect of the differences in average velocities, GPR data reach deeper depths through coarse sands with gravels.

This relationship between velocities of propagation of EM pulses and texture of sediments may be explained by the fact that fine sediments tend to retain higher water contents, especially when muds are present, increasing values of the material's dielectric permittivity. In turn, an increase in dielectric permittivity necessarily causes a decrease of the velocity of propagation of radio waves through the medium. In addition, in the environment studied, which has relatively high evapotranspiration rates throughout the year, coarse sandy materials tend to have high infiltration and evaporation rates, precluding the local retention of soilmoisture. As a result, the study's coarse sediments present lower dielectric constants and higher EM pulse propagation velocities (Figure 4).

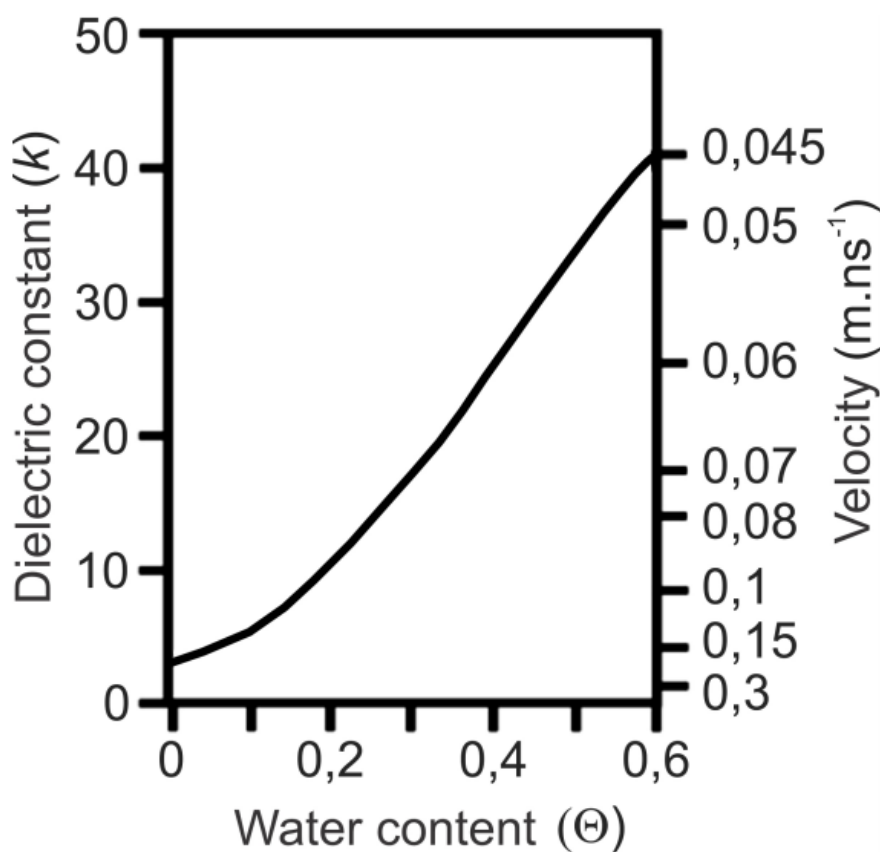


FIGURE 4

Basic relationships of geophysical properties for GPR surveys. The variation of water-content (#) in near-surface materials has an inversely proportional effect on dielectric permittivity values (#) and a directly proportional effect on the velocity of propagation of EM pulses (meters per nanoseconds).

Therefore, two groups of Quaternary materials are defined in this study by their geophysical properties: a) medium to fine sands, with low average velocities of propagation of GPR pulses; b) coarse sands and gravels, with high average velocities of propagation of GPR pulses. The massive structure that predominates in both deposits can be attributed to different causes, requiring further investigation (PETTIJOHN, 1987), such as: the temporal resilience of the diffuse pattern of transport and deposition that currently prevails across the Serra Branca valley; the rapid deposition that is common to flash flows; and the effects of subsequent pedogenesis on deposits.

The main distinction we would like to emphasize, however, is stratigraphic in nature: it concerns the prevailing opposition in our data between well-organized reflectors within Paleozoic sedimentary rocks and poorly-organized reflectors within Quaternary sediments. In addition, we note that the coarser Quaternary sediments, containing gravels, tend to present a better spatial organization of GPR reflectors, probably due to effects of a more variable granulometry.

OSL dating of deposits allows calculating sedimentation rates (Table 1). Dated deposits have been associated with some of the valley's geomorphological environments, which permits defining of either proximal or distal environments and respective sedimentation rates. In proximal environments, the sedimentation rates are higher at ramps within hollows than at the foot-slope of cliffs. This result can be attributed to higher uptake of precipitation that contributes to alluviation at sites with a basin morphology. In distal environments, the highest sedimentation rates occur within the lower Serra Branca valley, near its outlet, again in association with alluvial deposits. Deposits within a planation surface show the lowest

recorded sedimentation rates. Table 1 also indicates the dielectric permittivity and velocities of GPR pulse propagation within the dated materials.

Depth of dated sample	OSL Age (years)	Error (years)	Sedimentation rates (m.ky ⁻¹)	Environment *	Velocity (m.ns ⁻¹)	Dielectric Permittivity (F)
S-1: 67 cm	8.200	± 1,500	0,304	CR	0,119	6,30
S-2: 259 cm	8.240	± 1,070	0,383	CR	0,094	10,25
S-3: 300 cm	6.400	± 735	0,469	HR	0,168	3,17
S-4: 150 cm	23.860	± 3,230	0,147	EG	0,113	6,95
S-5: 190 cm	83.500	± 9,250	0,0067/0,047	EG	0,106	7,86
S-6: 510 cm	10.300	± 1,080	0,495	VO	0,195	2,35

TABLE 1
OSL dated samples and sedimentation rates, associated with environmental and geophysical characteristics of analyzed materials.

The geochronologic data indicate that proximal deposits, associated with sites adjacent to the cliffs surrounding the Sierra Branca Valley (CR and HR), accumulated during the Middle Holocene, or Northgripian substage (COHEN et al. 2018; WALKER et al., 2012), while distal deposits (VO and EG) came to rest during the Lower Holocene and the Upper Pleistocene, respectively near the valley outlet and across a planation surface.

The study's geochronological background, associated with the definition of either proximal or distal deposits, with recent ages occurring in proximal sites, suggests that the geomorphological evolution of the valley was driven by the lateral retreat of the surrounding cliffs, as would be expected for an area where pediments occur. This evolutionary hypothesis will be tested during the discussion of the following results.

Truncation surfaces and Holocene deposits on cliff foot-slopes

One of the GPR survey lines was materialized along a trail that runs parallel to the base of a cliff oriented irregularly SW-NE (radargrams 2 and 3 in Figure 2). The survey line is 970 meters long; moves away from the cliff while crossing the outlets of ramps (MEIS; MONTEIRO, 1979), in erosive amphitheaters, and approaches the cliff tangentially when crossing spurs. The bottom of the hollows has vegetation that is denser than the adjacent vegetation cover across the valley, where sands and rock outcrop, as shown in the orbital image (Figure 2). Results from two of those hollows are presented below.

The topographic profile along the trail indicates a gradual decrease in elevation to the NE, along approximately 366 meters, before reaching the studied hollow (Figure 5). The elevation then increases, as the track approaches the cliff spurs. A second hollow occurs at about 300 meters from the previous one. The topographic elevation continues to increase to the NE, down the valley (NNE), bordering the western cliffs. This gain in elevation towards downstream, contrary to the expected slope of the valley, is a consequence of a large amphitheater that was carved out of the western cliffs. The hollows and ramps studied are detailed features inside this large amphitheater (Figure 2). As the excavation of this large amphitheater seems to result from the cliff's retreat by back-wearing, the elevation tends to increase as the track extends into the relatively younger truncated outcrops to the NE. The general configuration of the terrain, to the WNW, is that of a higher topographic surface that gradually loses elevation towards the axis of the valley bottom, to the ESE, defining a gentle slope that is orthogonal to the NNE dip of local Paleozoic rocks (Figure 6). This configuration corroborates the hypothesis that was suggested earlier by geochronological data, according to which the younger hollows near the valley's cliffs result from back-wearing across an evolving planation surface.

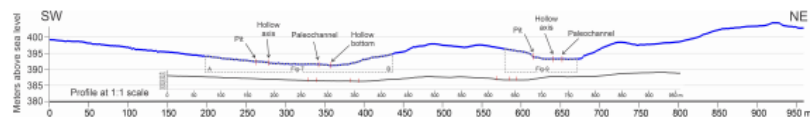


FIGURE 5

Topographic profile associated with a GPR survey line at the western edge of the Serra Branca valley. Note that the same topographic profile is illustrated, in black, without vertical exaggeration, below the figure's main profile, in blue. The segments highlighted by dashed rectangles indicate detailed sections associated with the radargrams of Figures 7 and 9. The arrows point to detailed features that are explained in the main text.



FIGURE 6

General aspect of the western portion of the Serra Branca valley, looking to the NNE. A gentle slope surface is highlighted, dipping towards the ESE (to the right). The slope extends out of sight into the background. Note the green aspect of the Caatinga vegetation, at the end of the rainy season.

Figure 7 illustrates a radargram along 243.5 meters of the survey line. The radargram was divided into two parts, for illustration (Figure 7.A and 7.B). Figure 7.A shows the characteristic pattern of GPR reflection that was previously defined, with strong magnitude reflectors associated with the sedimentary rocks, at greater depths, and low reflection zones associated with Quaternary formations, near the surface. Reflectors within rocks have a generally wavy distribution, dipping gently to the NE, parallel to the topographic surface across the first 35 meters of the radargram. Afterwards, the dip direction of reflectors is inverted to the SE for approximately 90 meters, until reaching the location of the topographic axis of the first hollow. At this point, high magnitude reflectors occur close to the topographic surface (Figures 2, 5 and 7.A). The change in dip direction of the basal reflectors along 55 meters gives the radar zone associated with the quaternary formations a lenticular geometry, which is reinforced by the decrease in thickness of the quaternary deposits to the NE. The remaining 30 meters of Figure 7.A, between 90 and 120 meters from the origin of the radargram, display relatively continuous high-reflectors near the surface, indicating the shallow depths of unconsolidated sediments covering sedimentary rocks.

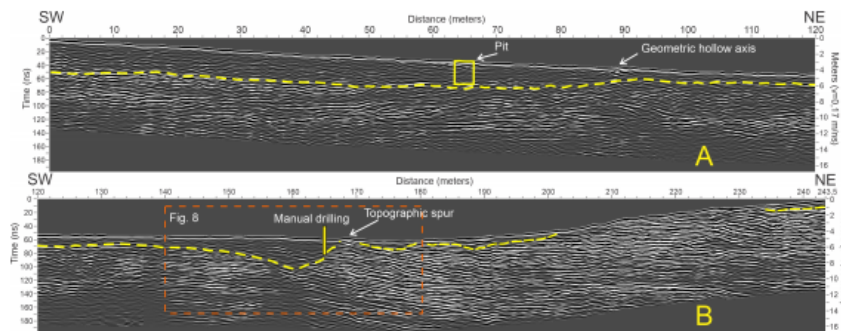


FIGURE 7

200 MHz radargram that partially crosses an ample system of erosive hollows at the western edge of the valley. The radargram is 243.5 meters long, and is positioned between 298 and 441.5 meters from the origin of the topographic profile (Figure 5). The orange dashed rectangle indicates the sector illustrated in Figure 8. Note the vertical exaggeration applied to the radargram topography.

Figure 7.B is the second half of the same radargram, showing that the Quaternary sediments start thickening at about 140 meters from the origin. Their thickness increases up to a depth of 4.7 meters at 160 meters from the radargram origin, and quickly decreases afterwards, delineating a channeled subsurface feature. The deposits that fill the NE edge of this channeled feature are arranged in disconformity over the high-magnitude reflectors in sandstones. The NE edge of the subsurface feature coincides with a small spur on the topographic surface, which also marks the transition to the rock outcrops that dominate the rest of the survey line (Figure 7.B). From this point, zones of thinner unconsolidated deposits occur, alternated with rock outcrops in which the GPR reflectors systematically end in an erosive truncation pattern beneath the topographic surface. Reflectors in sedimentary rocks end in tolap beneath the shallow Quaternary deposits. The whole set of GPR features points to the occurrence of a partially dissected and partially buried truncation surface of Holocene age (Table 1) that is exhumated at the final third of the radargram, northeastwards (Figure 7.B).

Figure 8 illustrates the channeled subsurface structure of Figure 7.B in detail, without vertical exaggeration, highlighting its main characteristics. Manual auger drilling was conducted 4.5 meters from the axis of the feature, and revealed that the transition between Holocene sands and Paleozoic rocks occur at a depth of 204 cm, confirming the GPR data and characterizing the feature as a cut-and-fill structure. A layer of sand with fine-gravels was identified between 172 cm and 202 cm below the surface, overlapping Paleozoic rocks.

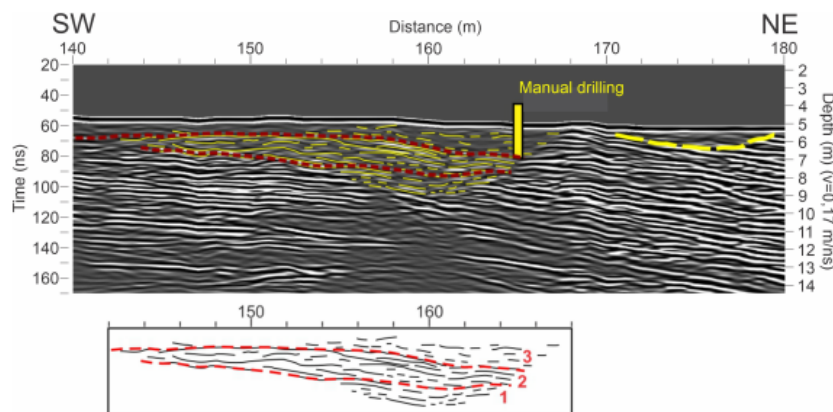


FIGURE 8

Illustration, without vertical exaggeration, of part of the radargram of Figure 7.B. The figure is centered on the asymmetric subsurface channeled structure. The main reflectors within the structure are highlighted in yellow. The bold red dashed lines mark the limits between different radar packages associated with allostratigraphic units. The inset, below, highlights the distribution of the GPR reflectors, and indicates the depositional order of the allostratigraphic units (red numbers).

The distribution of GPR reflectors (Figure 8) allows dividing the materials infilling the erosive incision into three units: 1) a lower unit, with GPR reflectors distributed parallel to the incision bottom, forming a 105 cm thick vertical-accretionary layer; 2) an intermediate unit, thoroughly sigmoidal, also with some sigmoidal inner reflectors that tend to be arranged in offlap, forming a 181 cm thick vertical and lateral-accretionary layer, probably associated with increasing sedimentation rates, with inputs of gravels; 3) a superior unit, displaying a semitransparent reflection pattern, with parallel to oblique discontinuous reflectors, associated with medium to coarse massive sands, composing a 187 cm thick layer. The general distribution of GPR reflectors within the Holocene deposits indicates the better organization and stronger signal of the deepest deposits (units 2 and 3), which are also better protected from the effects of pedogenesis. A more conclusive interpretation for these deposits depends on a detailed analysis of sediments and on complementary geochronological data.

The overall structure, however, suggests the accumulation of sediments associated with the migration of sedimentary inputs to the NE, as suggested by the offlap pattern of GPR reflectors in the intermediate unit, also in accordance with the asymmetry of the erosive incision (Figure 8). The results point to a 37-meter-wide and 4.7-meter-deep cut-and-fill structure, associated with the erosive incision of bedrocks along the paleo-axis of an erosive hollow. Deposits filling the incision were likely transported in a system similar to alluvial fans, building up three allostratigraphic units that were individualized by the GPR stratigraphic interpretation. A similar reflection pattern, also associated with cut-and-fill structures and truncation surfaces, can be observed in the radargram that crosses the second hollow along the survey line, farther to the NE (Figure 9 and Figure 5).

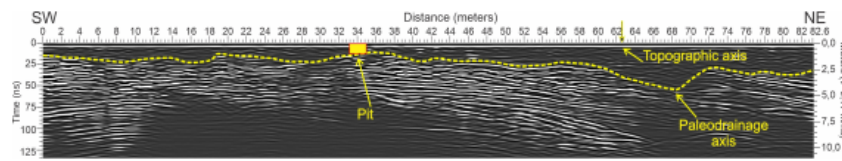


FIGURE 9
200 MHz radargram, crossing part of the second hollow outlet. Note that the radargram has no vertical exaggeration and was not corrected for topography.

A pit that was open at 95 meters to the SW from the axis of the first cut-and-fill structure (see Figure 7.A), near the topographic axis of the hollow, reveals a depositional pattern with some organization of GPR reflectors within the Quaternary formations, also at intermediate depths, as in the cut-and-fill structure. The pit is three meters deep and doesn't reach the bedrock. A transition between layers of massive coarse-sands and gravels is recorded at 210 cm and 230 cm below the topographic surface, defining the top and the base of a 20 cm thick layer of gravels. The depth of the layer of gravels and its thickness are equivalent to those found at the edge of the cut-and-fill structure discussed above. Sands found below and above the layer of gravels date from the Middle Holocene (Table 1, samples 1 and 2).

Taking into account the similarities between deposits and GPR features within the deposits of the two hollows, and observing that the dated sediments are not directly settled over the bedrocks, it is reasonable to assume that the onset of sedimentation in the cut-and-fill structures within the hollows is older than the Middle Holocene. We cannot claim that both paleo-incisions within the studied hollows have similar ages. Nor can we state that their ages are really older than the ages obtained within the pit. For now, the possibility that the hollows were incised earlier, either during the Lower Holocene or during the tardiglacial, remains as a working hypothesis for future research.

As a result, the GPR survey permits mapping subsurface structures that are genetically associated with the formation and evolution of hollows that were carved out of the cliffs that border the valley (Figure 2). The geomorphologic and stratigraphic setting indicates the occurrence of hollows and ramps that develop in a system of colluvial-alluvial lobes, bearing evidence of the incision of bedrocks along their topographic paleo-axis, where buried cut-and-fill structures are preserved. Deposits filling the incisions generate geophysical reflectors that indicate processes of vertical and lateral-accretion, and show a clear structural inner organization of sandy deposits. Within the hollow, the Quaternary deposits occur partially confined by truncated surfaces. The whole sector, therefore, may be defined as part of a dissected clastic pediment.

The sedimentary structures uncovered by the GPR survey challenge the common interpretation according to which the proximal deposits within the SCNP area would be exclusively colluvial in nature (OLIVEIRA et al., 2014). This generalization is based on the observation that deposits have a predominant massive sandy fraction. This is perfectly justifiable in cases where the sands compose the matrix of rudaceous deposits. However, sandy deposits are rarely massive and require a detailed sedimentological examination before confirming either the absence or presence of primary structures (PETTIJOHN et al., 1987; FERREIRA; OLIVEIRA, 2006). Our results show that relatively well-structured alluvial deposits occur at proximal sites, near the valley cliffs. In some cases, they occur confined within erosive paleo-incisions, in association with channeled-runoff (Figure 8).

The subsurface structure across this sector of the valley reinforces the hypothesis previously advanced on the basis of geochronological evidence, that the evolution of the Serra Branca valley bottom is controlled by an association between the dissection of bedrocks; the lateral retreat of cliffs that frame the valley, and the formation of partially buried and partially exposed Quaternary truncation surfaces, furthering a classic scenario for the production of planation surfaces evolving under the control of base level shifts.

Inversion of a pleistocenic thalweg and incision rates at the Serra Branca valley.

Figure 10 shows an altimetric profile obtained across a topographic remnant that extends in WSW-ENE direction, and that is interpreted as a flattened watershed. This profile is associated with 3,090 meters of GPR data, crossing the entire western portion of the Serra Branca valley, from the large amphitheater discussed above, crossing the valley's main thalweg, and extending over the eastern pediments (Figure 2, line GPR4). The profile perpendicularly traverses the northern slope of the flattened watershed. The segment of the profile that is highlighted in black in Figure 10, near the WNW border of the main thalweg, indicates the position of a GPR low-reflection zone that is illustrated in Figure 11. When viewed from the eastern cliffs of the valley, this lowered watershed recalls an erosive glacia (Figure 12).

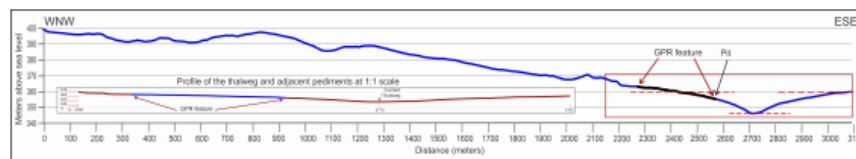


FIGURE 10

Topographic profile perpendicular to the northern slope of the razed watershed. Horizontal dashed red lines show the 14 to 19 meters-difference in elevation between the thalweg's bottom and the adjacent pediments. The inset below shows the profile across thalweg and pediments without vertical exaggeration. Note the position and extension of a GPR feature found below the western pediment surface.

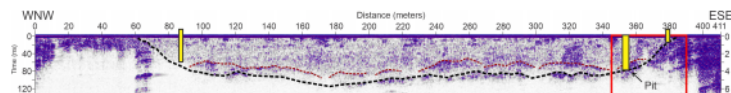


FIGURE 11

200 MHz radargrama showing a subsurface GPR feature that is associated with a 300 meters wide perched palaeochannel. The two yellow narrow bars indicate the positions of manual drillings. The wide yellow vertical bar indicates the position of a pit. The dashed red lines at across the bottom of the channel infillings are interpreted as lenses of gravels. The red rectangle near the ESE border of the channel refers to the area comprised by the radargram of Figure 14. Note the strong vertical exaggeration of this figure.

At approximately 2,270 m from the origin of the survey line, the radargram reveals a zone of low magnitude reflectors that extends for 315 meters to the ESE. This zone delineates a wide-channeled feature, 3.5 to 7.0 meters-deep, with a wavy bottom (Figure 11). The general relationship established in this study between magnitude and organization of GPR reflectors and subsurface materials, applies to this semitransparent GPR zone, associated with poorly reflective quaternary sediments, overlaying sediments and sedimentary rocks with high-magnitude GPR reflectors near the bottom, especially in the periphery of the feature. Unlike previous radargrams, however, the GPR signal across the zone becomes transparent at greater depths, virtually with no GPR signal. This indicates a strong attenuation of the EM signal with depth, probably in association with the diffusion of oxyhydroxides and/or clay-minerals within the deposits of the channeled feature. The spatial coincidence between the zone of EM signal attenuation and the channeled geometry assumed by the subsurface feature is remarkable.



FIGURE 12

General features of a razed watershed (left) and a near-cliff pediment (right, background) at the western border of the valley. The dashed yellow lines highlight the main profiles that give to the erosive remnants their glacial aspect. The white dashed lines indicate the local approximate limits of the perched paleochannel. The black arrow points to the lowered watershed's main divide.

A pit excavated near the ESE border of the feature confirms the relationship between the pattern of reflection and materials of the subsoil, revealing a 3.6-meter-thick package of massive medium to fine sands overlaying a 40-cm-thick layer of clast-supported polymodal gravels that cover weathered sandstones (Figure 13). Within this layer, the larger pebbles (between 5 and 10 cm) are well-rounded and predominantly oblate, with an average imbrication of 7° that is consistent with a NNE direction of deposition (penetrating to the right into the plane of Figure 13). OSL dating of sands above and below the layer of gravels indicates ages of 23.8 ka and 83.5 ka, respectively (Table 1, samples 4 and 5). Figure 14 illustrates the detailed structure of GPR reflection, highlighting the transition between the pleistocenic sands and gravels and the adjacent sedimentary rocks, near the area where the pit was excavated.

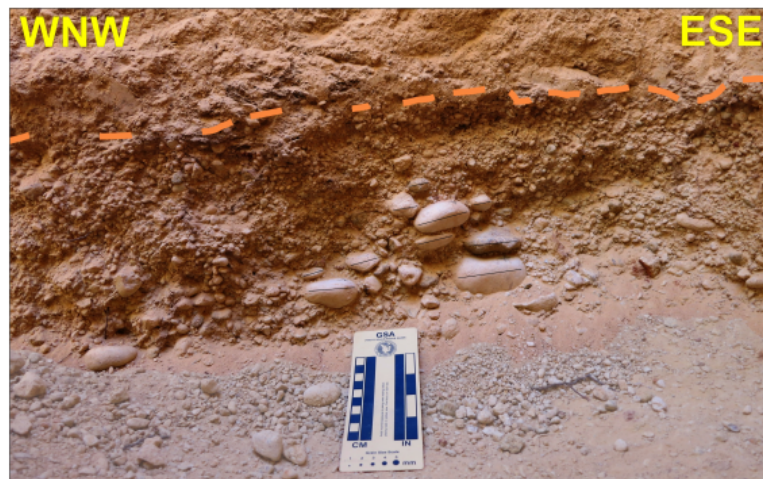


FIGURE 13

Layer of polymodal clast-supported gravels, with lenses of pebbles near the bottom of the pit. Note the orientation of the exposed main face of the pit, and the apparent imbrication of pebbles within the pit wall.

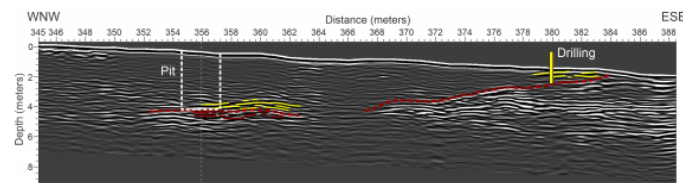


FIGURE 14

Detailed section of Figure 12 radargram. This 200 MHz radargram is illustrated without vertical exaggeration and was submitted to topographic correction. The reflectors highlighted in yellow point to deposits of gravels found in the field. Reflectors in red point to transitions between recent sediments and Paleozoic rocks. Note the inversion of direction of the dip of reflectors within the sands that overlay gravels and sedimentary rocks, at the vicinity and inside the area of the pit: the sand reflectors arrange in downlap over the rocks. The reflectors associated with sands, near the ESE border of the paleochannel, arrange in onlap upon the remnants of the channel's bank.

The contrast of the pattern of reflection between materials infilling the channeled feature and the sandstones below and adjacent to the ESE bank of the feature is evident, especially for the transitions between sediments and bedrocks (Figure 14). This pattern of GPR reflection occurs across the entire 315 meters of the feature, with packs of reflectors near the bottom of the paleochannel whose wavy configuration reproduce the lenticular geometry of the gravel deposits found at the bottom of the pit (Figures 12, 13 and 14).

As a result, all of the lenticular features observed in the radargram of Figure 11 are interpreted as similar lenses of gravels distributed across the pleistocenic channel. The general pattern of reflectors across the entire paleochannel suggests a fining-upward distribution of sediments, as indicated by the concentration of high-magnitude lenticular packages of reflectors in the lower portion of the deposits and by the gradually sparser high-magnitude reflection zones towards the top (Figure 11). As shown by the location of the feature in the topographic profile of Figure 10, the Pleistocene channel is positioned between 14 and 19 meters above the bottom of the current valley thalweg, indicating the occurrence of an abandoned perched channel, and its association with a process of local topographic inversion.

The ages obtained by OSL dating (Table 1) and the differences in elevation observed between the Pleistocene channel and the current thalweg axis indicate that the paleochannel was at work, and well-adapted to its local base-level, during the interstadial of Marine Isotopic Stage (MIS) 5a, about 83,500 years ago. As a result, the process of topographic inversion was triggered, at least, either during or after the Last Glacial Maximum (LGM), during or after the MIS 2, 23,860 years ago. The incision of the main valley thalweg to its current topographic position had probably forced the avulsion of the paleochannel and its abandonment. Since the current thalweg has no clearly defined river-channel across it, the general configuration of the pleistocenic channel, its size, and infilling deposits, suggest that runoff was more important, more frequent and more competent during the last glaciation than it is today. Between MIS 5 and MIS 2 running water formed a well-defined river-channel, probably braided, leaving bedload clast-supported rudaceous deposits within it (NICHOLS, 1999).

Considering the entire duration of the LGM, since the dated layer of gravels is overlaid by 3.5 meters of sands, the topographic inversion was driven by an average linear rate of incision of 0.74 meters per 1,000 years, or 0.74 mm.year⁻¹. This rate of incision is approximately two orders of magnitude smaller than river incision rates in humid temperate climate areas, such as Europe, for instance (SKARPICH et al. 2013), and is between one and two orders of magnitude higher than erosion rates verified in a desert environment (BIERMANN and CAFEE, 2001). As a result, our incision rate is theoretically consistent with the semiarid setting of the study area. The process of incision and topographic inversion was likely associated with the abandonment

of the paleochannel, probably by avulsion, preserving a channel relict more than 300 meters-wide under the gentle slope of lowered watershed. The wide and shallow paleochannel was probably braided (DIEZ-HERRERO et al., 2009). Today, there is no clearly incised channel, with well-defined banks (Montgomery and DIETRICH, 1988) across the lowest areas of the current Serra Branca valley thalweg. During the Upper Pleistocene, sediments were transferred by competent flows, confined in a fluvial channel.

Already with this interpretation in mind, when we were georeferencing the raw field data to produce the cartographic material, we noted that the pit that was excavated within the paleochannel deposits is located precisely at the edge of a linear outcrop that is situated on the eastern limits of a superficial feature that assumes a channeled geometry that is clearly visible in the plane of the orbital image used in Figure 2.

The linear outcrop was first interpreted as a residual ridge within the thalweg of the Serra Branca valley. During a subsequent field-survey we observed that the feature is composed of outcrops of sandstones covered by residual deposits of well-rounded gravels that are similar to the gravels found within the pit in the paleochannel deposits (Figure 13). These linear mounds of gravels and outcrops of sandstone are topographically perched above the current thalweg. Actually, their linear spatial distribution marks, along the valley thalweg, the edge of the erosive step that was created after the incision that was associated with the avulsion and abandonment of the pleistocenic channel. As a result, the subaerial gravel lags likely indicate the position of lateral bars of the abandoned pleistocenic braided channel. Moreover, the coincidence between the position and dimensions of the pleistocenic subsurface channel revealed by GPR data and those of the superficial channeled feature visible in the orbital image is conclusive (Figure 2). The feature shown in the orbital image is the remnant of a perched paleochannel that is about 300 meters-wide and 3,300 meters-long, at the studied area.

The orbital image of Figure 2 also indicates that the current thalweg, located to the ESE of the gravel lags, and the suspended paleochannel, both defined a zone of greener Caatinga vegetation across the valley bottom, when the orbital image was acquired. This zone of greener Caatinga vegetation is likely the result of differences in soil-water retention of near-surface sediments across the valley bottom. In areas covered by medium to fine sands, as found across the paleochannel remnants, the finer near-surface sediments allow for greater soil water retention, maintaining a greener local vegetation for longer periods after precipitation events. In the areas surrounding the paleochannel, across the planation surface and adjacent gravel lags, the Caatinga vegetation tends to be drier.

We should also emphasize the symmetry of the bottom of the current thalweg in the topographic profile of Figure 10, where its wide flattened “U” geometry may be observed. The current thalweg is bordered by two higher topographic steps, on both sides. These steps develop a classic topographic profile for pediments, with steeper shoulders near the thalweg and flattened surfaces at higher elevations. This geomorphic configuration supports our interpretation of a relatively recent incision of the current valley thalweg, and allows us to map the edges of at least two pediments that have been created since the LGM in the zone studied.

At this point, it is important to emphasize the consistency of our results, recalling the distinction initially made between grain-size of near-surface materials and their geophysical properties (Figure 4). The physical differences of sediments induce differences in dielectric permittivity of materials; differences in propagation velocities of EM pulses; hypothetical differences in soil water-content capacity, and differences of texture in orbital images. All these differences allow identifying and mapping deposits and landforms, present and past. The channeled feature that is observed in the orbital image corroborates all of the interpretations made in this work on the basis of the differences of GPR reflection patterns, which also illustrates the potential to apply the GPR methodology to geological and geomorphological mapping.

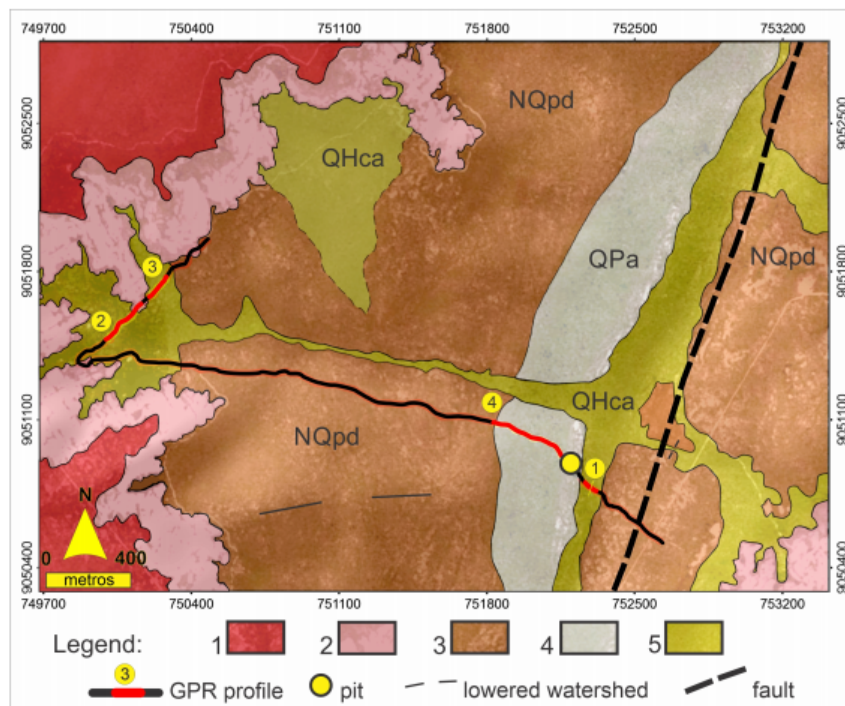


FIGURE 15

Geomorphological and geological map for the area. 1) Sandstone Plateau; 2) Cliffs; 3) NQpd: undifferentiated planation surfaces, of Neogene to Quaternary age; 4) QPa: Upper Pleistocene alluvial deposits, within a perched paleochannel; 5) QHca: colluvial-alluvial Holocene deposits, within amphitheaters, hollows and thalwegs. Data source: www.relevobr.cnpm.embrapa (accessed in: 10/11/2017). Metadata: UTM, Sirgas 2000,23 S.

Figure 15 presents a geological-geomorphological interpretation of the studied area, based on the spatialization of the main features that were identified by geophysical, geochronological and geomorphological evidences. As suggested by our results, we observe that the eastern side of the studied area presents a more fragmented planation surface. This configuration may be explained by the lateral migration of the current thalweg eastwards, since the abandonment of the pleistocenic channel, which shifted the drainage network towards the eastern cliffs of the valley, and allowed a better connection between erosion and sedimentation processes across the eastern pediments (OLIVEIRA; MEIS, 1985). OLIVEIRA, 1990). An opposite configuration applies to the hollows at the valley's western border. As shown in Figure 15, these hollows connect to the current thalweg only via a long and narrow through that crosses the perched pleistocenic channel, before it reaches the main current thalweg to the East. Note also that the deposits of a large amphitheater are equally mapped to the West. This site was studied only preliminarily, but its deposits appear to be disconnected from the main thalweg network, being perched on an attendant pediment. This large amphitheater is associated with the gain in elevation of the pediments to the NE (down the valley), as described earlier.

It is very likely that the process of incision of the planation surface, associated with the topographic inversion illustrated here, was caused by the adaptation of the pleistocenic runoff to a fault zone that is mapped near the eastern border of the current thalweg (Figure 15) (CPRM, 2009). This adaptation could force the avulsion of the pleistocenic channel eastwards, producing the valley's current thalweg. Further studies could clarify this problem properly, either defining whether this adaptation of base-level took place passively, as a result of differential erosion, or if it was actively induced by an eventual neo-tectonic adjustment.

CONCLUSIONS

Although this study employed relatively recent methods of geochronology and subsurface mapping, the results recall an original Brazilian geomorphological approach that was developed during the middle of the last century. This approach was focused on the observation of the relationship between landforms and correlated deposits (BIGARELLA; ANDRADE, 1965; BIGARELLA; MOUSINHO, 1965; BIGARELLA; MOUSINHO; SILVA, 1965; MEIS; MOURA, 1984). In our case study, this relationship emerges directly from the accumulated evidence, and provides material for a critical evaluation of the relationship between classic geomorphological theories and geological facts (PEULVAST; CLAUDINO SALES, 2003). Our results show a geomorphological setting that is consistent with these models, demonstrating the evolution and spatial distribution of Quaternary deposits and pediments under the control of local base-level adjustments. Considering the accumulated evidence, it is difficult to think of alternative interpretations for the detailed association between superficial structure (landforms), subsurface structure (deposits and rocks) and geochronology.

In another context, and in another continent, in the Sonoran-desert (USA), Larson et al. (2016) present geochronological results that also demonstrate the existence of periods of incision of pediments controlled by base level fluctuations. Although unaware of Professor Bigarella's original approach, the authors developed the concept of a "relict pediment surface" (op. Cit., P.1199), and use it to characterize and date stepped geomorphological surfaces. Obviously, the development and use of this concept by the authors represents an independent reinvention of classic Brazilian geomorphological models, illustrating how classic interpretations may be updated by the application of new methods, and that new methods do not necessarily imply new concepts.

In spite of the eventual resurgence of these models and concepts, the relationship between landforms and related deposits in northeastern Brazil still faces the challenge of finding sedimentologic and stratigraphic evidence that allow an unambiguous evaluation of the paleoclimatic implications of these classic approaches. In our case study in the Serra Branca valley, the position, dimensions, and deposits found within a pleistocene perched channel suggest that, although still probably semiarid, the local climate was wetter during the last glaciation than it is today. This wetter climatic condition apparently persisted for about 53,000 to 65,000 years, extending into the Last Glacial Maximum. Although the evidence of turbulent flows associated with this relict channel is quite consistent (bedload pebbles), challenging the classic cold-dry / warm-humid morphoclimatic binomial, the available data do not allow making a clear distinction between our results and the classic models of Brazilian geomorphology. Additional data is still required.

In any case, our results indicate that the Serra Branca valley bottom should be characterized as a partially dissected pediplane, whose remnants constitute dissected pediments that border the currentthalweg network. This characterization is in accord with all previous published geomorphological descriptions of the valley, which emphasize the flatness of the valley bottom, and make abundant references to its pediments, cliffs, etc.

We hope this study will be the first in a series focused on the definition of the spatial and temporal relationships between colluvial and alluvial deposits and the main geomorphic features within the Serra Branca pediplane. The study reveals subsurface structures that allow the formulation of evolutionary geomorphologic hypotheses and the definition of sedimentation and erosion rates compatible with the local and regional climates. The results also allow mapping detailed landforms and Quaternary alluvial deposits that have not been previously identified, updating the association between landforms and correlative deposits at the study area.

The application of the GPR methodology to the study of Quaternary deposits and to geological and geomorphological mapping allows highlighting some fundamental physical characteristics of materials and topographic surfaces; establishing sound relationships between deposits, rocks, landforms, aspects of

vegetation, texture of remote images, and landscape perception, whose convergence allows the definition of the spatial and interpretative order that underlies any attempt at mapping.

Finally, the study results led to the formulation of hypotheses and questions that we hope will inspire future research in the area. The geomorphologic interpretation enabled by the use of GPR methods and by the precision of RTK must still be refined through more detailed mapping, a better sedimentological characterization of colluvial and alluvial deposits, and with new geochronologic data, such as exposure dating of rocks and sediments. These are in progress, but will need complementary research programs. The area also needs a more detailed structural geological mapping to provide a better understanding of the eventual relationship between differential erosion and geotectonic influences.

ACKNOWLEDGEMENTS

We would like to thank the geologist Reginaldo Lemos for his generous participation on the acquisition and analysis of our data, for writing the review of the regional and local geology, and for his participation on the discussion of results. We also thank the Chico Mendes Institute for Conservation of Biodiversity (ICMbio); the Museum of the American Man Foundation (FUNDHAM); the Federal University at Vale do São Francisco (UNIVASF), and ACTUR Serra da Capivara for research permits and generous field support. We are also grateful to the National Council for Scientific and Technological Development (CNPq) for supporting the research projects, funded through processes 563307 / 2010-2; 476467 / 2013-6, and 459779 / 2014-1.

REFERENCES

- BARBOSA, R. C. M. Paleoambiente e proveniência da Formação Cabeças da Bacia do Parnaíba: evidências da glaciação famenniana e implicações na potencialidade do reservatório. 2012. 124 f. Tese nº 100 (Doutorado em Geologia) - Programa de Pós-Graduação em Geologia e Geoquímica, Universidade Federal do Pará, Belém.
- BARROS et al. Geoparque Serra da Capivara - PI, Projeto Geoparques, Proposta, CPRM, 54 p., 2011.
- BIERMAN, P. R.; CAFFEE, M. Slow rates of rock surface erosion and sediment production across the Namib desert an escarpment, Southern Africa. *American Journal of Science*, 301(4-5), pp. 326-358, 2001.
- BIGARELLA, J. J.; MOUSINHO, M. R.; SILVA, J. X. Pediplanos, pedimentos e seus depósitos correlativos no Brasil. *Boletim Paranaense de Geografia*, 16/17, pp. 117-154, 1965.
- BIGARELLA, J. J.; MOUSINHO, M. R. Considerações a respeito dos terraços fluviais, rampas de colúvios e várzeas. *Boletim Paranaense de Geografia*, 16/17, pp. 153-197, 1965.
- COHEN, K. M. et al. The ICS International Chronostratigraphic Chart. *Episodes*, 36(3), pp. 199-204, 2013 (2013; updated).
- CPRM (Serviço Geológico do Brasil). Projeto Borda Sudeste da Bacia Sedimentar do Parnaíba. Relatório I. Teresina, 2009. 153 p.
- CUNHA, F. M. B. Evolução Paleozóica da Bacia do Parnaíba e seu Arcabouço Tectônico. 1986. 107 f. Dissertação (Mestrado em Geologia) - Programa de Pós-Graduação em Geologia, Universidade Federal do Rio de Janeiro, Rio de Janeiro.
- DELLA FÁVERA, J. C. Tempestitos da Bacia do Parnaíba. Porto Alegre. 242 f. 1990. Tese de Doutorado. Tese (Doutorado em Geociências) - Programa de Pós-Graduação em Geociências, Instituto de Geociências/ Universidade Federal do Rio Grande do Sul.
- DÍEZ-HERRERO, A.; LAÍN-HUERTA; LLORENTE-ISIDRO, M. A handbook on flood hazard mapping methodologies. Madrid: Spanish Geological Survey, 2009. 190 p.
- DUNNE, T.; BLACK, R. D. Partial area contribution to storm runoff in a small New England watershed. *Water Resources Research*, 6(5), pp. 1296-1311, 1970.

- EMPERAIRE, L. La caatinga du sud-est du Piauí (Brésil) : Étude ethnobotanique. 327 f. 1980. Tese de Doutorado em Botânica Tropical - Université Pierre et Marie Curie-Paris VI, Paris, França.
- FERRAZ, N. C.; CÓRDOBA, V. C.; SOUZA, D. C. Análise estratigráfica da sequência mesodevoniana-eocarbonífera da Bacia do Parnaíba, nordeste do Brasil. *Geociências*, 36(1), pp. 154-172, 2017.
- FERREIRA, G. M. S. S.; OLIVEIRA, M. A. T. Aplicação da micromorfologia de solos ao estudo de sedimentos alúvio-colúviais em cabeceiras de vale. *Pesquisas em Geociências*, 33(2), pp. 2-18, 2006.
- GILBERT, G. K. Report on the geology of the Henry Mountains. Washington, DC: United States Geographical and Geological Survey of the Rocky Mountain Region, 1877. 160 p.
- GÓES, A. M. O.; FEIJÓ, F. J. Bacia do Parnaíba. *Boletim de Geociências da Petrobrás*, 8(1), pp. 57-68, 1994.
- KING, L. C. Canons of landscape evolution. *Geological Society of America Bulletin*, 64(7), pp. 721-752, 1953.
- KING, L. C. The morphology of the Earth. Edinburgh: Oliver and Boyd, 1967. 726 p.
- LARSON, P. H. et al. Pace of landscape change and pediment development in the Northeastern Sonoran Desert, United States. *Annals of the American Association of Geographers*, 106(6), pp. 1195-1212, 2016.
- MESNER, J. C.; WOOLDRIDGE, L. C. Estratigrafia das bacias paleozóica e mesozóica do Maranhão. *Boletim Técnico da Petrobrás*, 2(7), pp. 137-164, 1964.
- MEIS, M. R. M.; MONTEIRO, A. M. F. Upper Quaternary “rampas”, Doce River Valley, Southeastern Brazilian Plateau. *Zeitschrift für Geomorphologie*, 23(2), pp. 132-151, 1979.
- MEIS, M. R. M.; MOURA, J. R. S. Upper Quaternary sedimentation and hillslope evolution: Southeastern Brazilian Plateau. *American Journal of Science*, 284(3), pp. 241-254, 1984.
- MONTGOMERY, D. R.; DIETRICH, W. E. Where do channels begin? *Nature*, 336(6169), pp. 232-234, 1988.
- NICHOLS, G. *Sedimentology and Stratigraphy*. Oxford: Blackwell Science, 2000. 355 p.
- OLIVEIRA, P. E. et al. Paleoclimas da Caatinga brasileira durante o Quaternário tardio. In: CARVALHO, I., S. et al. (Org.) *Paleontologia: cenários da vida – Paleoclimas*. Rio de Janeiro: Editora Interciência, 2014. p. 501-516.
- OLIVEIRA, M. A. T. Slope geometry and gully erosion development: Bananal, São Paulo, Brazil. *Zeitschrift für Geomorphologie*, 34(4), pp. 423-434, 1990.
- OLIVEIRA, M. A. T.; MEIS, M. R. M. Relações entre geometria do relevo e formas de erosão acelerada, Bananal, São Paulo. *Geociências*, São Paulo, 4(1), pp. 87-99, 1985.
- OLIVEIRA, M. A. T.; PORSANI, J. L.; LIMA, G. L.; JESKE-PIERUSCHKA, V.; BEHLING, H. Upper Pleistocene to Holocene peatland evolution in Southern Brazilian highlands as depicted by radar stratigraphy, sedimentology and palynology. *Quaternary Research*, 77(3), pp. 397-407, 2012.
- PELLERIN, J. Les bases physiques. In : GUIDON, N. (Org.) *L'aire archéologique du sud-est du Piauí*. Paris : Recherche sur les Civilisations, 1984. p. 11-22.
- PEULVAST, J. P.; CLAUDINO SALES, V. Stepped surfaces and paleolandforms in the Northern Brazilian “Nordeste”: constraints on models of morphotectonic evolution. *Geomorphology*, 62(1) pp. 89-122, 2003.
- PETTIJOHN, F. J.; POTTER, P. A.; SIEVER, R. Sand and sandstone. 2. ed. New York: Springer-Verlag, 1987. 553 p.
- PROCHOROFF, R.; BRILHA, J. Preliminary study in Serra da Capivara National Park (Piauí, Brazil): integrating geological and archaeological heritage in a world heritage site. In: HILARIO, A. et al. (Org.) *Patrimonio geológico y geoparques, avances de um caminho para todos*. Madrid: Instituto Geológico y Minero de España, Cuadernos del Museo Geominero (18), 2015. p. 43-46.
- SANTOS, J. C. O Quaternário do Parque Nacional Serra da Capivara e entorno, Piauí, Brasil: morfoestratigrafia, sedimentologia, geocronologia e paleoambientes. 2007. 182 f. Tese (Doutorado em Geociências) – Programa de Pós-Graduação em Geociências, Universidade Federal de Pernambuco, Recife.
- SANTOS, J. C.; BARRETO, A. M. F.; SUGUIO, K. Quaternary deposits in the Serra da Capivara National Park and surrounding area, Southeastern Piauí state, Brazil. *Geologia USP. Série Científica*, 12(3), pp. 115-132, 2012.
- SKARPICH, V.; HRADECKÝ, J.; DUSEK. Complex transformation of the geomorphic regime of channels in the forefield of the Moravskoslezské Beskydy Mts.: Case study of the Morávka River (Czech Republic). *CATENA*, 111, pp. 25-40, 2013.

- TWIDALE, C. R. Pediments, peneplains, and ultiplains. *Revue de Geomorphologie Dynamique* 32, pp. 1–38, 1983.
- TWIDALE, C. R.; BOURNE, J. A. Episodic exposure of inselbergs: *Geological Society of America Bulletin*, 86(10), pp. 1473–1481, 1975.
- TWIDALE, C. R.; BOURNE, J. A. Do pediplains exist? Suggested criteria and examples. *Zeitschrift für Geomorphologie*, 57(4), pp. 411–28, 2013.
- VAZ, P.T. et al. Bacia do Parnaíba. *Boletim de Geociências da Petrobras*, 15, pp. 253-263, 2007.
- WALKER, M.J.C. et al. Formal subdivision of the Holocene Series/Epoch: a discussion paper by a Working Group of INTIMATE (Integration of ice-core, marine and terrestrial records) and the Subcommission on Quaternary Stratigraphy (International Commission on Stratigraphy). *Journal of Quaternary Science*, 27(7), pp.649–659, 2012.